Manipulation of tripartite-to-bipartite entanglement localization under quantum noises and its application to entanglement distribution

Xin-Wen Wang,[1,2,*] Shi-Qing Tang,[2] Ji-Bing Yuan,[2] and Le-Man Kuang[2,†]
[1]*Department of Physics and Electronic Information Science, Hengyang Normal University, Hengyang 421002, China*
[2] *Key Laboratory of Low-Dimensional Quantum Structures and Quantum Control of Ministry of Education, and Department of Physics, Hunan Normal University, Changsha 410081, China*

This paper is to investigate the effects of quantum noises on entanglement localization by taking an example of reducing a three-qubit Greenberger-Horne-Zeilinger (GHZ) state to a two-qubit entangled state. We consider, respectively, two types of quantum decoherence, i.e., amplitude-damping and depolarizing decoherence, and explore the best von Neumann measurements on one of three qubits of the triple GHZ state for making the amount of entanglement of the collapsed bipartite state be as large as possible. The results indicate that different noises have different impacts on entanglement localization, and that the optimal strategy for reducing a three-qubit GHZ state to a two-qubit one via local measurements and classical communications in the amplitude-damping case is different from that in the noise-free case. We also show that the idea of entanglement localization could be utilized to improve the quality of bipartite entanglement distributing through amplitude-damping channels. These findings might shed a new light on entanglement manipulations and transformations.

PACS numbers: 03.67.Bg, 03.67.Pp, 03.65.Yz, 03.67.Mn
Keywords: Entanglement distribution, entanglement localization, GHZ state, decoherence

arXiv:1402.1914v2 [quant-ph] 16 Jan 2015

I. INTRODUCTION

Establishment of entanglement among distant parties is a prerequisite for implementing lots of remote quantum-information processing tasks [1, 2]. In situations of practical interest, most of these scenarios involve many parties, and the specific subsets which will carry out quantum communications are not known when the entangled resources are generated and distributed among all of the parties. Particularly, different nodes in a quantum network are usually connected by multipartite entangled states [3, 4], and the two-party quantum communication protocols between any two possible parities are not set in advance. For accomplishing two-party quantum communications, they need to previously establish bipartite entanglement between them via the help of other parties [5]. It is hence interesting to search efficient ways to extract entangled states with fewer particles (e.g., two particles) from multiparticle entangled states.

Many theoretical works study, as a method of establishing entanglement between two of many parties who previously share a multipartite entangled state, a reduction the multipartite entangled state to a bipartite entangled state via local measurements assisted by classical communications. Such a paradigm of localizing bipartite entanglement is related to the notions of entanglement-of-assistance [6, 7], localizable-entanglement [8, 9], and entanglement-of-collaboration [10]. They quantify the maximal average amount of entanglement of two parties that can be extracted from a multipartite entangled state via (local) measurements and different ways of classical communications. From the practical point of view, however, it may be more important to maximize the entanglement between the chosen two parties for specific events, where the desired measurement outcomes of other parties are gotten, as shown in this paper.

The idea of entanglement localization works perfectly for ideally isolated systems. In practice, however, no system can be completely isolated from surroundings [11], and the system will experience decoherence because of the interaction with environment. Multipartite entanglement, which holds much richer quantum correlations than bipartite entanglement, is known to be very fragile to decoherence and to display subtle decay features [12–15], especially when an entangled multiparticle state is distributed into several distant recipients [4, 16]. Then the conventional entanglement localization strategies may achieves no longer the optimization. Therefore, it is important to understand and optimize techniques to realize effective entanglement localization in the face of noise and decoherence.

In this paper, we investigate the effects of quantum noises on the tripartite-to-bipartite entanglement localization and the optimal single-particle measurement strategy for reducing a three-qubit Greenberger-Horne-Zeilinger (GHZ) state [17] to a two-qubit entangled state. We show that the amplitude and depolarizing noises have different impacts on entanglement localization, and that the best von Neumann measurement on one of three qubits of a triple GHZ state for extracting a two-qubit entangled state in the amplitude-damping environment is different from that in the noise-free and depolarizing cases. These results indicate that when considering the amplitude-damping decoherence, the three parties who previously share a three-qubit GHZ state should take different entanglement localization strategy from that in the ideal case, for increasing the amount of entanglement of the final two-qubit entangled state. In addition, we also demonstrate that the idea of entanglement localization could be utilized to improve the quality of bipartite entanglement distribution.

The paper is organized as follows. In section II, we describe the process of entanglement localization from a three-qubit GHZ state to a two-qubit entangled state and give the optimal measurement basis of anyone of the three qubits. In section III, we show how can the idea of entanglement localization boost the quality of bipartite entanglement distribution. Concluding remarks are given in section IV.

*xwwang@mail.bnu.edu.cn
†lmkuang@hunnu.edu.cn

II. TRIPARTITE-TO-BIPARTITE ENTANGLEMENT LOCALIZATION UNDER QUANTUM NOISES

GHZ states, typical multipartite maximally entangled states, are usually employed for entanglement distribution among different nodes of a quantum network [18, 19], due to the fact that they can be used to implement numerous quantum information protocols [1, 2]. On the other hand, the characteristics of a GHZ state with many bodies could be usually obtained by straightforwardly generalizing that of tripartite GHZ states [20–23]. In consequence of these facts, we here focus on entanglement localization of tripartite GHZ states. Considering the case that Alice, Bob, and Charlie, staying far away from each other, previously share a three-qubit GHZ state

$$|\psi\rangle^{(123)} = \frac{1}{\sqrt{2}}(|000\rangle + |111\rangle)_{123}, \tag{1}$$

where $\{|0\rangle, |1\rangle\}$ is the computational basis of a qubit. Qubits 1, 2, and 3 are in the labs of Alice, Bob, and Charlie, respectively. Now two of them, e.g., Alice and Bob, want to implement private quantum communication with the existing quantum resource, the GHZ-type entangled state. To this end, they need to first establish bipartite entanglement between them through the assistance of the third party, Charlie. The easiest and robust method is that Charlie performs a local measurement on qubit 3 and broadcasts the outcome, this is so called entanglement localization [8, 9]. Ideally, that is, in the noise-free case, the best measurement that Charlie should adopt is a projective measurement with basis $\{|\pm\rangle = (|0\rangle \pm |1\rangle)/\sqrt{2}\}$, because Alice and Bob can attain a maximally entangled state, the Bell state $|B_+\rangle^{(12)} = (|00\rangle + |11\rangle)_{12}/\sqrt{2}$ or $|B_-\rangle^{(12)} = (|00\rangle - |11\rangle)_{12}/\sqrt{2}$, for each possible measurement outcome, $|+\rangle$ or $|-\rangle$. As a matter of fact, the average amount of entanglement between Alice and Bob is one being equivalent to the localizable-entanglement allowed in this case [8, 9]. The procedure of the entanglement localization is schematically sketched in Fig. 1 (a).

In practice, qubits 1, 2, and 3 will undergo independently decoherence induced by local noises, and the canonical GHZ state will be converted into a mixed state before we preforming the entanglement localization procedure, as shown in Fig. 1 (b). We first consider the amplitude noise [24] in section A, and then discuss other noise models, e.g., depolarizing model [24], in section B.

A. Entanglement localization under amplitude-damping decoherence

Amplitude-damping decoherence is suited to many practical qubit systems, including vacuum-single-photon qubit with photon loss, atomic qubit with spontaneous decay, and superconducting qubit with zero-temperature energy relaxation. The action of amplitude noise can be described by two Krauss operators,

$$K_0 = \begin{pmatrix} 1 & 0 \\ 0 & \sqrt{\bar{d}} \end{pmatrix}, \quad K_1 = \begin{pmatrix} 0 & \sqrt{d} \\ 0 & 0 \end{pmatrix} \tag{2}$$

with $0 \leqslant d \leqslant 1$ and $\bar{d} = 1 - d$. K_1 describes the transition of $|1\rangle$ to $|0\rangle$, while K_0 describes the evolution of the system without such a transition. Note that $d = 0$ denotes the noise-free case and $d = 1$ means the interactional time or strength between the system and environment tending to infinity. Therefore, the decoherence strength d is acquiesced in the range $(0, 1)$ in the following discussion.

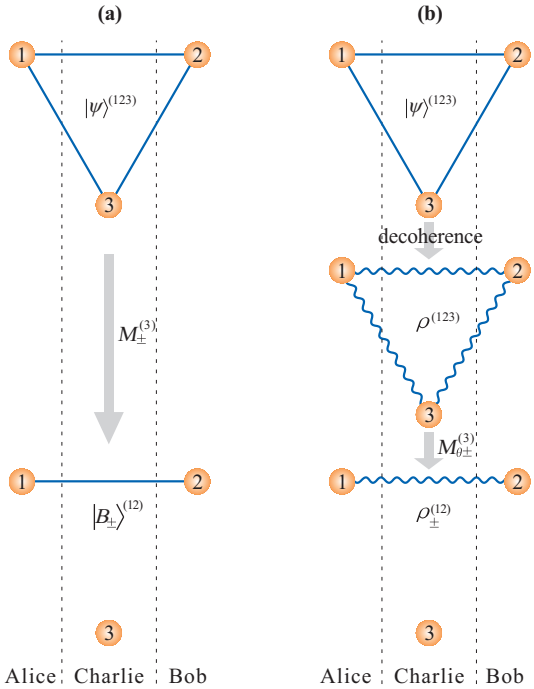

FIG. 1: (Color online) Sketch map of entanglement localization for the initial three-qubit GHZ state. Diagram **(a)** describes the ideal case where the system is isolated perfectly from its surroundings and does not suffer from decoherence; diagram **(b)** describes the case where each qubit undergoes decoherence before the performance of entanglement localization protocol. The qubits that are linked by straight lines are in a maximally entangled pure state, and that are linked by wave lines are in a mixed state. $M_{\theta\pm}^{(3)}$ ($M_{\pm}^{(3)}$) denotes a von Neumann measurement on qubit 3 with projectors $M_{\theta+}^{(3)} = |+_\theta\rangle_3\langle+_\theta|$ ($M_{+}^{(3)} = |+\rangle_3\langle+|$) and $M_{\theta-}^{(3)} = |-_\theta\rangle_3\langle-_\theta|$ ($M_{-}^{(3)} = |-\rangle_3\langle-|$), where the measurement basis $\{|+_\theta\rangle, |-_\theta\rangle\}$ is given in Eq. (4).

After each qubit interacting with a local amplitude-damping environment, the standard GHZ state in Eq. (1) degenerates to a mixed state

$$\begin{aligned}
\rho^{(123)} &= \sum_{l,m,n=0}^{1} K_l \otimes K_m \otimes K_n |\psi\rangle^{(123)}\langle\psi| K_l^+ \otimes K_m^+ \otimes K_n^+ \\
&= \frac{1}{2}(1 + d_1 d_2 d_3)|000\rangle\langle 000| + \frac{1}{2}\bar{d}_1\bar{d}_2\bar{d}_3|111\rangle\langle 111| \\
&\quad + \frac{1}{2}\sqrt{\bar{d}_1\bar{d}_2\bar{d}_3}|000\rangle\langle 111| + \frac{1}{2}\sqrt{\bar{d}_1\bar{d}_2\bar{d}_3}|111\rangle\langle 000| \\
&\quad + \frac{1}{2}d_1 d_2\bar{d}_3|001\rangle\langle 001| + \frac{1}{2}d_1\bar{d}_2 d_3|010\rangle\langle 010| \\
&\quad + \frac{1}{2}\bar{d}_1 d_2 d_3|100\rangle\langle 100| + \frac{1}{2}d_1\bar{d}_2\bar{d}_3|011\rangle\langle 011| \\
&\quad + \frac{1}{2}\bar{d}_1 d_2\bar{d}_3|101\rangle\langle 101| + \frac{1}{2}\bar{d}_1\bar{d}_2 d_3|110\rangle\langle 110|,
\end{aligned} \tag{3}$$

where d_1, d_2, and d_3 denote the decoherence strengths of qubits 1, 2, and 3, respectively. For helping Alice and Bob to establish a two-qubit entangled state with as much entanglement as possible, Charlie needs to make a suitable local mea-

surement on qubit 3 and informs them of the outcome. We here only pay attention to the von Neumann measurement. The general single-qubit projective measurement basis can be described by

$$\begin{aligned} |+_\theta\rangle &= \cos\frac{\theta}{2}|0\rangle + \sin\frac{\theta}{2}e^{i\varphi}|1\rangle, \\ |-_\theta\rangle &= \sin\frac{\theta}{2}e^{-i\varphi}|0\rangle - \cos\frac{\theta}{2}|1\rangle, \end{aligned} \tag{4}$$

where $\theta \in [0,\pi]$ and $\varphi \in [0,2\pi]$. When $\theta = \pi/2$ and $\varphi = 0$, $|\pm_\theta\rangle$ reduce to $|\pm\rangle$. The probability of getting the outcome $|+_\theta\rangle_3$ is given by

$$\begin{aligned} P_+(d,\theta) &= \mathrm{Tr}\left[|+_\theta\rangle_3\langle+_\theta|\rho^{(123)}\right] \\ &= \frac{1}{2} + \frac{d_3}{2}\cos\theta. \end{aligned} \tag{5}$$

The occurrence of this event will lead to the fact that qubits 1 and 2 are projected in the state

$$\begin{aligned} \rho_+^{(12)} &= \frac{1}{P_+}\mathrm{Tr}_3\left[|+\rangle_3\langle+|\rho^{(123)}\right] \\ &= \frac{1}{P_+}\left(\gamma_+|00\rangle\langle 00| + \kappa_+|01\rangle\langle 01| + \tau_+|10\rangle\langle 10|\right. \\ &\quad \left.+\eta_+|11\rangle\langle 11| + \xi|00\rangle\langle 11| + \xi^*|11\rangle\langle 00|\right), \end{aligned} \tag{6}$$

where

$$\begin{aligned} \gamma_+ &= \frac{1}{2}(1+d_1d_2d_3)\cos^2\frac{\theta}{2} + \frac{1}{2}d_1d_2\bar{d}_3\sin^2\frac{\theta}{2}, \\ \kappa_+ &= \frac{1}{2}d_1\bar{d}_2d_3\cos^2\frac{\theta}{2} + \frac{1}{2}d_1\bar{d}_2\bar{d}_3\sin^2\frac{\theta}{2}, \\ \tau_+ &= \frac{1}{2}\bar{d}_1d_2d_3\cos^2\frac{\theta}{2} + \frac{1}{2}\bar{d}_1d_2\bar{d}_3\sin^2\frac{\theta}{2}, \\ \eta_+ &= \frac{1}{2}\bar{d}_1\bar{d}_2d_3\cos^2\frac{\theta}{2} + \frac{1}{2}\bar{d}_1\bar{d}_2\bar{d}_3\sin^2\frac{\theta}{2}, \\ \xi &= \frac{1}{2}\sqrt{\bar{d}_1\bar{d}_2\bar{d}_3}\sin\frac{\theta}{2}\cos\frac{\theta}{2}e^{i\varphi}. \end{aligned} \tag{7}$$

If the measurement outcome on qubit 3 is $|-_\theta\rangle_3$, which happens with probability

$$\begin{aligned} P_-(d,\theta) &= \mathrm{Tr}\left[|-\rangle_3\langle-|\rho^{(123)}\right] = 1 - P_+(d,\theta) \\ &= \frac{1}{2} - \frac{d_3}{2}\cos\theta, \end{aligned} \tag{8}$$

qubits 1 and 2 will be projected in the state

$$\begin{aligned} \rho_-^{(12)} &= \frac{1}{P_-}\mathrm{Tr}_3\left[|-\rangle_3\langle-|\rho^{(123)}\right] \\ &= \frac{1}{P_-}\left(\gamma_-|00\rangle\langle 00| + \kappa_-|01\rangle\langle 01| + \tau_-|10\rangle\langle 10|\right. \\ &\quad \left.+\eta_-|11\rangle\langle 11| - \xi|00\rangle\langle 11| - \xi^*|11\rangle\langle 00|\right), \end{aligned} \tag{9}$$

where

$$\begin{aligned} \gamma_- &= \frac{1}{2}(1+d_1d_2d_3)\sin^2\frac{\theta}{2} + \frac{1}{2}d_1d_2\bar{d}_3\cos^2\frac{\theta}{2}, \\ \kappa_- &= \frac{1}{2}d_1\bar{d}_2d_3\sin^2\frac{\theta}{2} + \frac{1}{2}d_1\bar{d}_2\bar{d}_3\cos^2\frac{\theta}{2}, \\ \tau_- &= \frac{1}{2}\bar{d}_1d_2d_3\sin^2\frac{\theta}{2} + \frac{1}{2}\bar{d}_1d_2\bar{d}_3\cos^2\frac{\theta}{2}, \\ \eta_- &= \frac{1}{2}\bar{d}_1\bar{d}_2d_3\sin^2\frac{\theta}{2} + \frac{1}{2}\bar{d}_1\bar{d}_2\bar{d}_3\cos^2\frac{\theta}{2}. \end{aligned} \tag{10}$$

Next, we use two measures, negativity [25, 26] and fully entangled fraction (FEF) [27, 28], to quantify the entanglement of $\rho_+^{(12)}$ and $\rho_-^{(12)}$, respectively, and analyze their features. Negativity has been considered as a dependable measure of entanglement for bipartite entangled states [25, 26]. FEF, which expresses the purity of a bipartite mixed state, plays a central role in quantum teleportation and entanglement distillation [27–30], and may behave differently from negativity as shown later.

1. *Negativity of the collapsed state of qubits 1 and 2*

Following Ref. [25], we use the following definition of negativity:

$$N(\rho) = \max\left\{0, -2\lambda_{\min}(\rho)\right\}, \tag{11}$$

with $\lambda_{\min}$ the minimal eigenvalue of the partial transpose of ρ denoted as ρ^T. After straightforward calculations we obtain the negativity of $\rho_+^{(12)}$ and $\rho_-^{(12)}$ as

$$N_+(\rho_+) = \max\left\{0, -2\mu_+\right\}, \tag{12}$$

$$N_-(\rho_-) = \max\left\{0, -2\mu_-\right\}, \tag{13}$$

where μ_+ and μ_- are, respectively, the minimal eigenvalues of ρ_+ and ρ_-, given by

$$\mu_+ = \frac{1}{2P_+}\left(\kappa_+ + \tau_+ - \sqrt{(\kappa_+ - \tau_+)^2 + 4|\xi|^2}\right), \tag{14}$$

$$\mu_- = \frac{1}{2P_-}\left(\kappa_- + \tau_- - \sqrt{(\kappa_- - \tau_-)^2 + 4|\xi|^2}\right). \tag{15}$$

For clarity, we give a detailed analysis on N_+ and N_- for the case $d_1 = d_2 = d_3 = d$ (which is not a necessary assumption but only simplifies the degree of algebraic complexity). In this case, μ_+ and μ_- reduce, respectively, to

$$\mu_+^s = \frac{\bar{d}}{2P_+}\left(d^2\cos^2\frac{\theta}{2} + d\bar{d}\sin^2\frac{\theta}{2} - \sqrt{\bar{d}}\,\sin\frac{\theta}{2}\cos\frac{\theta}{2}\right) \tag{16}$$

$$\mu_-^s = \frac{\bar{d}}{2P_-}\left(d^2\sin^2\frac{\theta}{2} + d\bar{d}\cos^2\frac{\theta}{2} - \sqrt{\bar{d}}\,\sin\frac{\theta}{2}\cos\frac{\theta}{2}\right) \tag{17}$$

The clear dependence of N_+ and N_- on d and θ is plotted in Fig. 2.

It can be seen from Fig. 2 that when d increases to a threshold, being away from one, for a given θ, both N_+ and N_- decrease to zero. This indicates that the entanglement vanishes in a finite time, which is referred to as entanglement sudden death [31–35]. More interesting and important information that can be obtained from Fig. 2 is as follows. If $d = 0$ (corresponding to the absence of noise), both of N_+ and N_- attain their maximal values at $\theta = \pi/2$, meaning that $\{|\pm\rangle_3\}$ is the optimal measurement basis. This result is in accordance with the discussion before. For $d > 0$, however, both N_+ and N_- are asymmetric with respect to $\theta = \pi/2$ in the region that d is less than the threshold defined above. This feature implies that N_+ and N_- reach their maximums at the points that deviate from $\theta = \pi/2$, respectively. Such phenomena can be observed clearly in Fig. 3 which gives the bivariate functions $\Delta N_+(d,\theta) = N_+(d,\theta) - N_+(d,\theta = \pi/2)$ and $\Delta N_-(d,\theta) = N_-(d,\theta) - N_-(d,\theta = \pi/2)$ with independent variables θ and d. We can see that there exist different regimes of θ in which ΔN_+ and ΔN_- are larger than

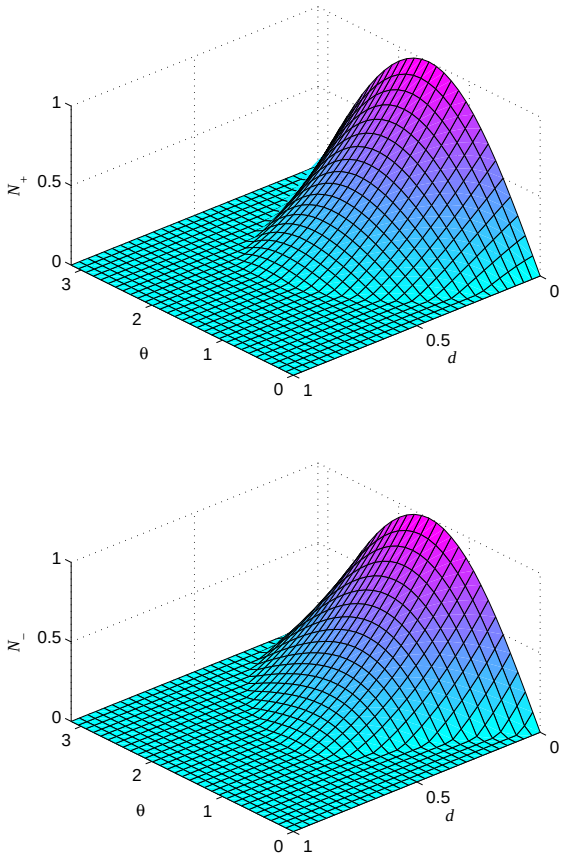

FIG. 2: (Color online) The function graph of N_+ and N_- with respect to d and θ.

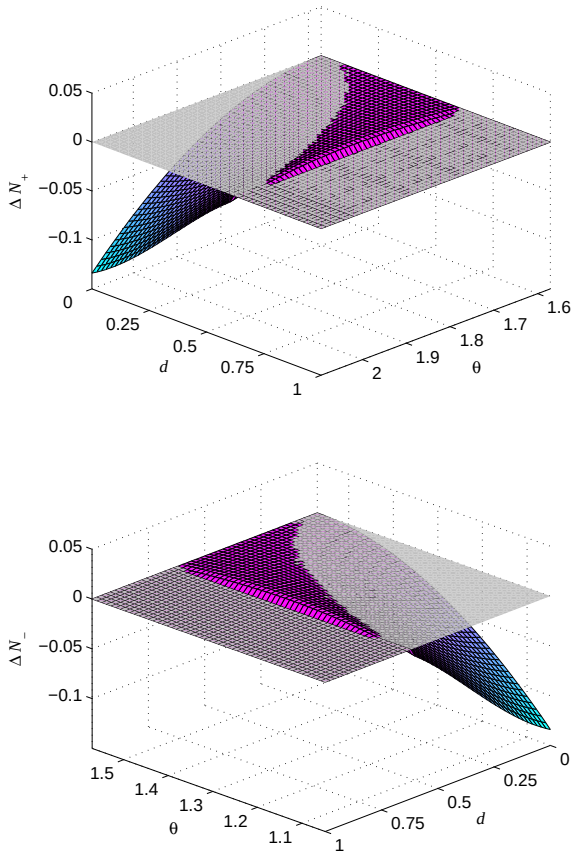

FIG. 3: (Color online) The dependence of ΔN_+ and ΔN_- on d and θ, where θ ranges from $\pi/2$ to $2\pi/3$ in the upper graph and from $\pi/3$ to $\pi/2$ in the lower graph.

zero, respectively; that is, $N_+(d, \theta \neq \pi/2)$ and $N_-(d, \theta \neq \pi/2)$ are indeed larger than $N_+(d, \pi/2)$ and $N_-(d, \pi/2)$, respectively. These results indicate that Charlie can enhance probabilistically the entanglement distributed between Alice and Bob by selecting an appropriate measurement basis $\{|+_{\theta\neq\pi/2}\rangle, |-_{\theta\neq\pi/2}\rangle\}$ instead of $\{|+\rangle, |-\rangle\}$.

The average amount of entanglement between qubits 1 and 2 for two possible measurement outcomes $|+_\theta\rangle$ and $|-_\theta\rangle$ is given by

$$N_{\rm ave}(d, \theta) = P_+ N_+ + P_- N_-. \tag{18}$$

It can be easily verified that when d is smaller than a threshold, the maximal value of $N_{\rm ave}(d, \theta)$ is $N_{\rm ave}(d, \pi/2)$ for a given d. When d goes beyond the threshold, however, $N_{\rm ave}(d, \theta)$ can attain its maximum at two different values of θ, situating symmetrically on the two sides of $\theta = \pi/2$, provided that $N_{\rm ave}(d, \theta)$ is not always equal to zero, as shown in Fig. 4; this fact means that $\{|\pm\rangle\}$ is no longer the optimal measurement basis of qubit 3. Figure 4 also indicates that the existing time of the entanglement of the state ρ_+ or ρ_- can be protracted by taking an appropriate measurement basis $\{|+_{\theta\neq\pi/2}\rangle, |-_{\theta\neq\pi/2}\rangle\}$ instead of $\{|+\rangle, |-\rangle\}$.

In the discussion above, we supposed that everyone of three qubits suffer decoherence. The obtained result is naturally applicable to special cases. That is, when only one or two qubits sustain decoherence, the optimal measurement basis of qubit 3 is also not $\{|+\rangle, |-\rangle\}$. Let us take an example of $d_3 = 0$ and $d_1 = d_2 = d$. Then N_+ and N_- in

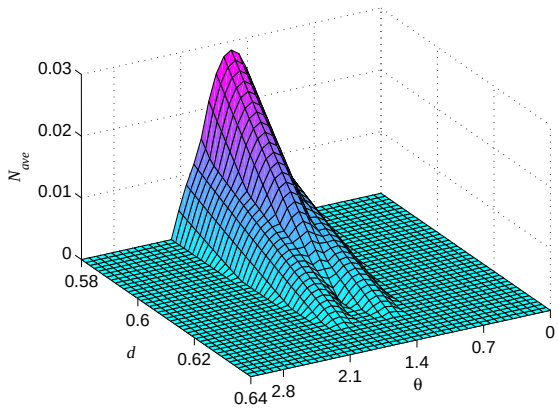

FIG. 4: (Color online) $N_{\rm ave}$ versus d and θ. The figure only plots the region of $0.58 \leqslant d \leqslant 0.64$.

Eqs. (12) and (13) reduce, respectively, to

$$N_+ = \max\left\{0,\ 2\bar{d}\sin\frac{\theta}{2}\left(\cos\frac{\theta}{2} - d\sin\frac{\theta}{2}\right)\right\}, \tag{19}$$

$$N_- = \max\left\{0,\ 2\bar{d}\cos\frac{\theta}{2}\left(\sin\frac{\theta}{2} - d\cos\frac{\theta}{2}\right)\right\}, \tag{20}$$

Evidently, the points of maximum of both N_+ and N_- are not at $\theta = \pi/2$. That is to say, the best measurement basis of

qubit 3 is not $\{|+\rangle, |-\rangle\}$ in the aforementioned entanglement localization protocol.

2. FEF of the collapsed state of qubits 1 and 2

FEF of a state ρ is defined as the maximum overlap of ρ with a maximally entangled state [27, 28], that is,

$$F(\rho) = \max_{|\phi\rangle} \langle\phi|\rho|\phi\rangle, \tag{21}$$

where the maximization is taken over all maximally entangled states $|\phi\rangle$. For two-qubit systems $F(\rho)$ can be analytically expressed as [36]

$$F(\rho) = \frac{1}{4}\left\{1 + \mu_1 + \mu_2 - \mathrm{sgn}[\det(\tilde{R})]\mu_3\right\}, \tag{22}$$

where $\{\mu_i\}$ are the decreasingly ordered singular values of the 3×3 real matrix $\tilde{R} = [\mathrm{tr}(\rho\sigma_i \otimes \sigma_j)]_{3\times 3}$ with $\{\sigma_i, i = 1, 2, 3\}$ the Pauli matrices and $\mathrm{sgn}[\det(\tilde{R})]$ is the sign of the determinant of $\tilde{R}$.

The FEF of the states ρ_+ and ρ_- in Eq. (6) and Eq. (9) can be calculated to be

$$F_+(\rho_+) = \frac{1}{4} + \frac{(4|\xi| + \gamma_+ + \eta_+ - \kappa_+ - \tau_+)}{4P_+}, \tag{23}$$

$$F_-(\rho_-) = \frac{1}{4} + \frac{(4|\xi| + \gamma_- + \eta_- - \kappa_- - \tau_-)}{4P_-}. \tag{24}$$

As before, we still discuss the case $d_1 = d_2 = d_3 = d$. Then $F_+(\rho_+)$ and $F_-(\rho_-)$ reduce, respectively, to

$$F_+(d, \theta) = \frac{1}{2} - \mu_+^s, \tag{25}$$

$$F_-(d, \theta) = \frac{1}{2} - \mu_-^s. \tag{26}$$

Then the FEF F_+ and F_- have the similar behaviors to the negativity N_+ and N_-, respectively. That is, F_+ and F_- reach their maximal values at $\theta \neq \pi/2$. As a matter of fact, F_+ (F_-) and N_+ (N_-) have the same extremal point, and there exist the same scale of d in which $F_+(d, \theta)$ [$F_-(d, \theta)$] and $N_+(d, \theta)$ [$N_-(d, \theta)$] are larger than $F_+(d, \theta = \pi/2)$ [$F_-(d, \theta = \pi/2)$] and $N_+(d, \theta = \pi/2)$ [$N_-(d, \theta = \pi/2)$], respectively. Thus Charlie can also increase the FEF of the state shared by Alice and Bob by adopting a suitable measurement basis $\{|+_{\theta\neq\pi/2}\rangle, |-_{\theta\neq\pi/2}\rangle\}$ instead of $\{|+\rangle, |-\rangle\}$.

The mean value of F_+ and F_- can be calculated as

$$\begin{aligned} F_{\mathrm{ave}} &= P_+F_+ + P_-F_- \\ &= \frac{3}{8} + \sqrt{\bar{d}_1\bar{d}_2\bar{d}_3}\sin\frac{\theta}{2}\cos\frac{\theta}{2} + \frac{1}{8}(2d_1 - 1)(2d_2 - 1). \end{aligned} \tag{27}$$

For $d_1 = d_2 = d_3 = d$, F_{ave} reduces to

$$F_{\mathrm{ave}}(d, \theta) = \frac{3}{8} + \bar{d}\sqrt{\bar{d}}\,\sin\frac{\theta}{2}\cos\frac{\theta}{2} + \frac{1}{8}(2d - 1)^2. \tag{28}$$

Obviously, the maximal value of $F_{\mathrm{ave}}(d, \theta)$ is $F_{\mathrm{ave}}^{\max}(d) = F_{\mathrm{ave}}(d, \theta = \pi/2)$ which is independent of the parameter θ. This result indicates that F_{ave} has different behavior to $N_{\mathrm{ave}}(d, \theta)$ which reaches the maximal value at $\theta \neq \pi/2$ when d oversteps a critical value (see Fig. 4).

In view of practice, however, what we are interested in is to maximize F_+ or F_-, due to the fact that the larger the FEF is, the higher teleportation fidelity and entanglement purification efficiency can be achieved [27–30]. Moreover, we notice that if and only if the FEF of a two-qubit state ρ is larger than 1/2, quantum teleportation can exhibit its superiority over state estimation based on classical strategies and entanglement purification can be carried out effectively using the resource state ρ [27–30]. We observe that $F_{\mathrm{ave}}(d, \theta) \leqslant 1/2$ does not mean $F_+(d, \theta)$ and $F_-(d, \theta)$ are simultaneously less than $1/2$. In deed, when $d \geqslant \left(\sqrt{5} - 1\right)/2$, $F_{\mathrm{ave}}^{\max} \leqslant 1/2$ [obtained from Eq. (28)], indicating that the resource state is useless for quantum teleportation and entanglement distillation, while $F_+(d, \theta > \pi/2)$ or $F_-(d, \theta < \pi/2)$ can overtop $1/2$ as displayed in Fig. 5. Thus we could safely conclude that when we take the measurement strategy that maximizes F_{ave}, both ρ_+ and ρ_- may be useless for quantum teleportation and entanglement distillation; in contrast, if we select an appropriate measurement basis $\{|\pm_{\theta\neq\pi/2}\rangle\}$ rather than $\{|\pm\rangle\}$ such that $F_{\mathrm{ave}} < F_{\mathrm{ave}}^{\max}$, Alice and Bob can implement effective teleportation and entanglement distillation with a nonzero probability. In other words, $\{|\pm\rangle_3\}$ is not the best measurement basis for optimizing the robustness of the entangled state of qubits 1 and 2.

It has been mentioned before that maximizing the average amount of entanglement between two particles of a multiparticle state by performing local measurements on the other particles is defined as localizable-entanglement [8, 9]. The conclusions presented above imply that localizable-entanglement is not suitable to be described by the entanglement measure of FEF from the practical point of view.

Although FEF may be not monotonic in the regime of small values under trace-preserving local operations and classical communication (TPLOCC) for mixed states [36–39], the aforesaid conclusions are reliable as explained below. The expressions of FEF in Eq. (25) and Eq. (26) can be rewritten as

$$F_+(d, \theta) = \begin{cases} \frac{1}{2}(1 - 2\mu_+^s) & \text{for } N_+ = 0 \ (\mu_+^s \geqslant 0), \\ \frac{1}{2}(1 + N_+) & \text{for } N_+ > 0 \ (\mu_+^s < 0), \end{cases} \tag{29}$$

$$F_-(d, \theta) = \begin{cases} \frac{1}{2}(1 - 2\mu_-^s) & \text{for } N_- = 0 \ (\mu_-^s \geqslant 0), \\ \frac{1}{2}(1 + N_-) & \text{for } N_- > 0 \ (\mu_-^s < 0). \end{cases} \tag{30}$$

It is well known that TPLOCC cannot create entanglement and thus cannot increase N_+ or N_-. Then, TPLOCC cannot increase F_+ or F_- in the present case because of the relationships given in Eqs. (29) and (30), which is in accordance with the result of Ref. [40]. In fact, both states ρ_+ and ρ_- do not belong to the class of states presented in Refs. [36, 37] whose FEF may be slightly raised by TPLOCC operations. The same argument could be obtained for the results in the following context. Thus we will not consider the local manipulations on qubits 1 and 2 and the classical communications between Alice and Bob themselves later.

B. Entanglement localization under depolarizing decoherence

In the former subsection, we have shown that the optimal strategy for extracting a two-qubit entangled state

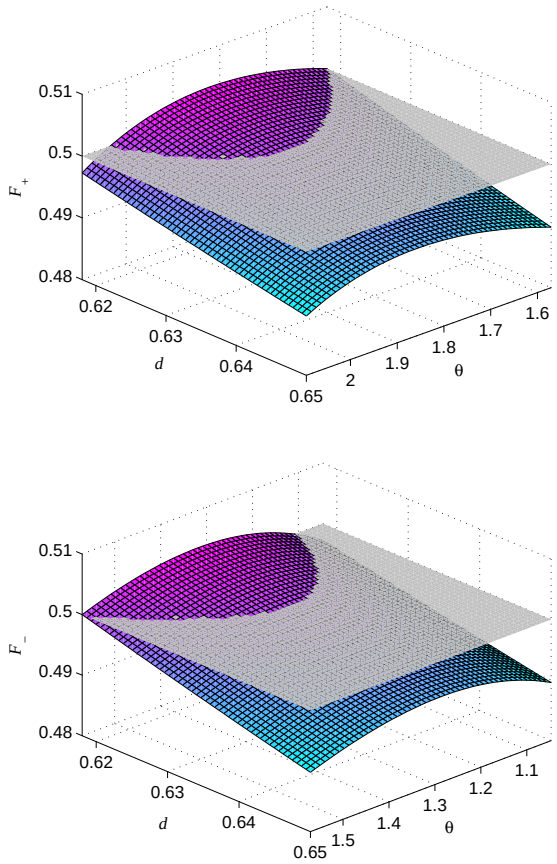

FIG. 5: (Color online) F_+ and F_- versus d and θ, where d is in the range $[(\sqrt{5}-1)/2, 0.65]$ and θ is in the range $[\pi/2, 2\pi/3]$ for the upper diagram and $[\pi/3, \pi/2]$ for the lower diagram.

from a three-qubit GHZ state via local measurements in the amplitude-damping case is different from that in the noise-free case. Particularly, in the ideal case, the best measurement basis of qubit 3 for reducing the three-qubit GHZ state $|\psi\rangle^{(123)}$ to a two-qubit entangled state $\rho^{(12)}$ is $\{|+\rangle_3, |-\rangle_3\}$; while considering the amplitude-damping decoherence of part or all of these qubits, the best measurement basis of qubit 3 is no longer $\{|+\rangle_3, |-\rangle_3\}$. This phenomenon does not necessarily occur under other noise models. We here take an example of depolarizing model.

The single-qubit depolarizing channel is described as

$$\mathcal{E}(\rho) = \sum_{i=0}^{3} p_i \sigma_i \rho \sigma_i \tag{31}$$

where ρ is the input state of the qubit, $p_0 = 1 - d$ and $p_i = d/3$ $(i = 1, 2, 3)$ with d being the degree of decoherence $(0 \leq d \leq 1)$, σ_0 is the identity operator, and $\{\sigma_i\}$ $(i = 1, 2, 3)$ are the Pauli operators σ_x, σ_y, σ_z, respectively.

For the initial three-qubit GHZ state $|\psi\rangle^{(123)}$ in Eq. (1), the depolarizing operation on each qubit will result in it becoming

$$\rho'^{(123)} = \sum_{i,j,k=0}^{3} p_i p_j p_k \sigma_i \otimes \sigma_j \otimes \sigma_k |\psi\rangle\langle\psi| \sigma_i \otimes \sigma_j \otimes \sigma_k. \tag{32}$$

Without loss of generality, we consider that the degree of decoherence of every qubit is not zero. For simplicity, we suppose the qubits have the same degree of decoherence d. After the aforementioned entanglement localization process, the negativity of the final state of qubits 1 and 2 is

$$\mathcal{N} = \max\{0, -2\lambda\}, \tag{33}$$

where $\lambda = 2(3-2d)d/9 - |3-4d|^3 \sin\theta/54$ for both the measurement outcomes $|+_\theta\rangle_3$ and $|-_\theta\rangle_3$ of qubit 3. In order to guarantee $\mathcal{N} > 0$, the condition

$$\sin\theta > \frac{12(3-2d)d}{|3-4d|^3} \tag{34}$$

should be satisfied. Then the point of maximum of $\mathcal{N}$ is at $\theta = \pi/2$ for any d. Moreover, the condition of Eq. (34) in the case $\theta = \pi/2$ can be satisfied more easily than in the case $\theta \neq \pi/2$. Thus, the optimal measurement basis of qubit 3 is $\{|+_{\theta=\pi/2}\rangle = |+\rangle, |-_{\theta=\pi/2}\rangle = |-\rangle\}$. Similarly, using the entanglement measure of FEF, the same conclusion can be obtained. In a word, the optimal strategy for reducing a three-qubit GHZ state to a two-qubit entangled state via local measurements in the depolarizing case is the same as that in the noise-free case.

The results above indicate that depolarizing and amplitude-damping noises have different effects on entanglement localization. It tells us that in different environments, we should take different strategies for optimizing the entanglement localization schemes.

III. BIPARTITE ENTANGLEMENT DISTRIBUTION ASSISTED BY THREE-PARTICLE ENTANGLED STATES

Inspired by the afore-cited phenomena in section II, we find that multiparticle entangled states could help to improve the quality of entanglement distribution between two distant parties in noisy environments, as demonstrated in this section.

A routine way of bipartite entanglement distributing between two distant parties, Alice and Bob, is to generate a two-qubit entangled state, e.g., a Bell state, in a server, say Charlie, and then physically send the two qubits to the labs of Alice and Bob, respectively. We here propose another way that first preparing a three-qubit entangled state, GHZ state, in Charlie's site and then send any two qubits, e.g., qubits 1 and 2, to Alice and Bob, one person one qubit, followed by the entanglement localization procedure introduced in the former section. In the noise-free case, the two methods will achieve the same result in terms of the shared entanglement between Alice and Bob. However, when considering the unavoidable effect of noises on the systems during their transmission, the latter scheme could boost probabilistically the amount of entanglement of the two-qubit state shared by Alice and Bob, as shown below. For clarity, the first method will be called direct distribution scheme, DDS for short, and the second one will be referred to as ancilla-assisted distribution scheme abbreviated to ADS. The schematic diagrams of both DDS and ADS are sketched in Fig. 6. The detailed descriptions on the DDS and ADS are given in sections A and B, respectively.

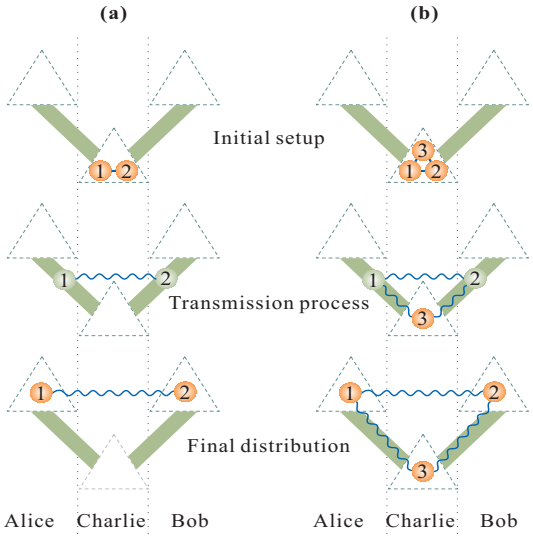

FIG. 6: (Color online) Two schemes for distributing bipartite entanglement. **(a)** Direct distribution scheme (DDS). **(b)** Ancilla-assisted distribution scheme (ADS), where the process of entanglement localization is not shown in the diagram and the detailed description on it is given in the context (see also Fig. 1). The green bars denote the quantum channels with which Charlie sends particles 1 and 2 to Alice and Bob, respectively. Linking the qubits by beelines denote that these qubits are in a maximally entangled pure state, while linking the qubits by wave lines denote these qubits being in a mixed state.

A. DDS for distributing bipartite entanglement via noisy quantum channels

In order to display the advantages of ADS later, we first recapitulate the results of DDS for providing a sharp contrast. Suppose that qubits 1 and 2 are initially prepared in a Bell state

$$|\phi\rangle_{12} = \frac{1}{\sqrt{2}}(|00\rangle + |11\rangle)_{12}. \tag{35}$$

After the two qubits independently interacting with their environments via amplitude-damping channels, the Bell state evolves into a mixed state

$$\begin{aligned}\varrho_{12} &= \sum_{m,n=0}^{1} K_m \otimes K_n |\phi\rangle_{12}\langle\phi| K_m^+ \otimes K_n^+ \\ &= \frac{1}{2}(1+d_1d_2)|00\rangle\langle 00| + \frac{1}{2}\bar{d}_1\bar{d}_2|11\rangle\langle 11| \\ &\quad + \frac{1}{2}\sqrt{\bar{d}_1\bar{d}_2}|00\rangle\langle 11| + \frac{1}{2}\sqrt{\bar{d}_1\bar{d}_2}|11\rangle\langle 00| \\ &\quad + \frac{1}{2}d_1\bar{d}_2|01\rangle\langle 01| + \frac{1}{2}\bar{d}_1 d_2|10\rangle\langle 10|. \end{aligned} \tag{36}$$

The negativity and FEF of ϱ can be calculated, respectively, to be

$$N(\varrho) = \max\{0, -2\lambda_{\min}(\varrho)\}, \tag{37}$$

$$\lambda_{\min} = \frac{1}{4}\left(d_1\bar{d}_2 + \bar{d}_1 d_2\right) - \frac{1}{4}\sqrt{(d_1-d_2)^2 + 4\bar{d}_1\bar{d}_2},$$

$$F(\varrho) = \frac{1}{4}\left(2 + 2\sqrt{\bar{d}_1\bar{d}_2} + 2d_1d_2 - d_1 - d_2\right). \tag{38}$$

We assume $d_1 = d_2 = d$, that is, the decoherence strengths of both qubits are the same. This is not a necessary assumption but only simplifies the degree of algebraic complexity, which makes no difference to the final conclusion. Then $N(\varrho)$ and $F(\varrho)$ reduce to

$$N'(\varrho) = (1-d)^2, \tag{39}$$

$$F'(\varrho) = \frac{1}{2}(1+N'). \tag{40}$$

B. ADS for distributing bipartite entanglement via noisy quantum channels

Some results in Sec. II can be transplanted to this section for simplifying the discussion on the ADS of bipartite entanglement distribution. It is observed from Sec. II that the negativity and FEF of the states ρ_+ and ρ_- are symmetric about $\theta = \pi/2$. Thus we here only discuss the entanglement properties of ρ_+, and the counterparts for ρ_- can be directly obtained using the symmetry.

Following Eq. (12) and Eq. (23), when $d_1 = d_2 = d$, $N_+(\rho_+)$ and $F_+(\rho_+)$ reduce to

$$N'_+(\rho_+) = \max\left\{0, \frac{2}{P_+}\left(|\xi'| - \kappa'_+\right)\right\}, \tag{41}$$

$$F'_+(\rho_+) = \begin{cases} \frac{1}{2} + \frac{1}{P_+}\left(\kappa'_+ - |\xi'|\right) & \text{for } N_+ = 0, \\ \frac{1}{2}(1+N'_+) & \text{for } N_+ > 0, \end{cases} \tag{42}$$

where

$$\kappa'_+ = \frac{d\bar{d}}{2}\left(d_3\cos^2\frac{\theta}{2} + \bar{d}_3\sin^2\frac{\theta}{2}\right),$$

$$|\xi'| = \frac{\bar{d}}{2}\sqrt{\bar{d}_3}\sin\frac{\theta}{2}\cos\frac{\theta}{2}. \tag{43}$$

We now make a comparison between the aforementioned two strategies, DDS and ADS, by analyzing the differences of the negativity and FEF of the state ρ_+ with that of the state ϱ, which are given by

$$\delta N = N'_+(\rho_+) - N'(\varrho), \tag{44}$$

$$\delta F = F'_+(\rho_+) - F'(\varrho). \tag{45}$$

What we are interested in is whether δN and δF could be larger than zero. This expectation is possible if and only if $N'_+(\rho_+) > 0$ and $F'_+(\rho_+) > 1/2$. According to Eqs. (39)-(42), it can be acquired that δN and δF have the same behavior in the regime of $N'_+(\rho_+) > 0$ and $F'_+(\rho_+) > 1/2$. Thus we only need to analyze the characteristics of δN, with which the features of δF can also be derived straightforwardly.

To exhibit ADS's superiority clearly, we first assume $d_3 = 0$, meaning that qubit 3 is well isolated from the noisy environment in Charlie's lab. In this case, the dependence of δN on d and θ is given in Fig. 7 with $0 \leqslant \theta \leqslant \pi/2$. When $\pi/2 < \theta \leqslant \pi$, $\delta N \leqslant 0$ (i.e., $N'_+ \leqslant N'$) for all d. Figure 7 shows that δN can be indeed larger than zero, i.e., $N'_+(\rho_+) > N'(\varrho)$, in a large region of d and θ. More importantly, when d is very large and close to one, meaning the quantum channels are very noisy and the coherence of the transmitted particles degenerate heavily, $N'_+(\rho_+)$ can overstep $N'(\varrho)$ in almost all the range $0 < \theta < \pi/2$. As a matter of fact, the larger d is, the larger range of θ is allowed to be selected for ensuring $\delta N > 0$. It implies that the larger d is,

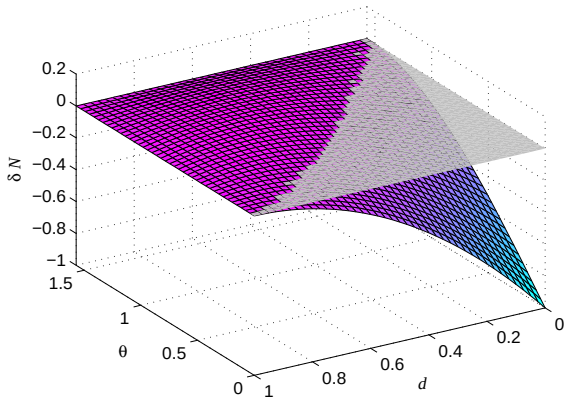

FIG. 7: (Color online) δN as a function of d and θ, where θ ranges from 0 to $\pi/2$.

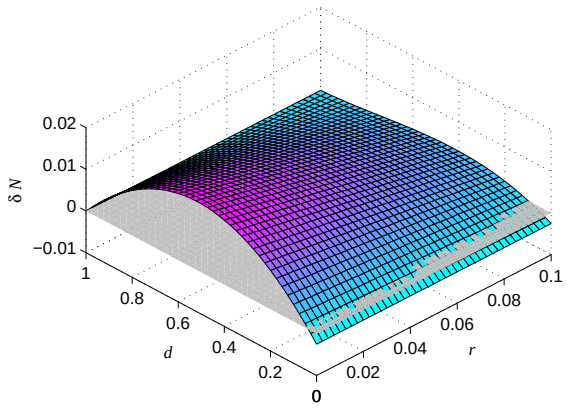

FIG. 8: (Color online) δN versus d and r ($= d_3/d$), where $r \in [0, 0.1]$ and $\theta \equiv \theta' = 1/5$.

the more flexible the ADS is. Moreover, if we take a measurement angle θ' that is slightly less than $\pi/2$, $N'_+(\rho_+)$ is nearly always larger than $N'(\varrho)$.

As to $d_3 > 0$, we only consider d_3 is very small relative to d, due to the fact that qubit 3 is not transmitted remotely. That is to say, the ratio of d_3 to d is far less than unit. On the other hand, it has been pointed out that if one selects a measurement angle θ' which is close to but less than $\pi/2$, $N'_+(\rho_+)$ is larger than $N'(\varrho)$ for almost the whole regime of $0 < d < 1$. Based on these considerations, we plot δN as a function of d and $r = d_3/d$ in Fig. 8 with $\theta \equiv \theta' = 1.5$ and $0 \leqslant r \leqslant 0.1$. It can be seen that even when d_3 takes nonzero values, $N'_+(\rho_+)$ can be larger than $N'(\varrho)$ for almost all values of d. It is worth pointing out that the increase in d_3 will lead to the increase in the probability P_+ of obtaining the state $\rho_+^{(12)}$ for a fixed θ, because P_+ is proportional to the product of d_3 and $\cos\theta$ as given in Eq. (5). Now we can safely conclude that the aforementioned ADS is able to enhance, with a certain probability, the quality of bipartite entanglement distribution, compared to DDS in the above-mentioned case.

IV. CONCLUDING REMARKS

In summary, we have investigated the effect of quantum decoherence on the localization of a three-qubit GHZ state to a two-qubit entangled state. We used two different entanglement measures, negativity and FEF, to quantify the resulting bipartite entanglement after localization procedure. It turns out that the optimal measurement basis in the noise-free case is no more the optimal one under the amplitude noise. Moreover, the depolarizing noise has different influence from amplitude noise on the entanglement localization. The difference of the effects and the change of the optimal measurement bases justify the necessity of investigating the entanglement localization in various noisy environments. It has also been shown that the optimal measurement basis in the concept of localizable-entanglement does not match to the one for optimizing the practical applications of entanglement localization. Furthermore, we found that the idea of entanglement localizing could be used to probabilistically improve the equality of bipartite entanglement distribution. These findings shed new insights into entanglement manipulations and transformations, and provide a new idea of entanglement distributing against decoherence as well.

Although the results above are obtained from the case that the initial multipartite entangled resource is a three-qubit GHZ state, the conclusions could be directly generalized to the case involving N-qubit ($N > 3$) GHZ states. It is deserved to research the effects of different types of quantum noises on entanglement localization and distribution for a variety of multipartite entangled states.

Acknowledgments

This work was supported by the China Postdoctoral Science Foundation funded project (Grant No. 2013T60769 and No. 2012M511729), the NSFC (Grant No. 11004050 and No. 11375060), the 973 Program (Grant No. 2013CB921804), the Hunan Provincial Natural Science Foundation (Grant No. 2015JJ3029), the Hunan Provincial Applied Basic Research Base of Optoelectronic Information Technology (Grant No. GDXX007), and the construct program of the key discipline in Hunan province.

[1] Horodecki R, Horodecki P, Horodecki M and Horodecki K 2009 *Rev. Mod. Phys.* **81** 865-942
[2] Pan J W, Chen Z B, Lu C Y, Weinfurter H, Zeilinger A and Żukowski M 2012 *Rev. Mod. Phys.* **84** 777-838
[3] Acín A, Cirac J I and Lewenstein M 2007 *Nature Phys.* **3** 256-259
[4] Kimble H J 2008 *Nature* **453** 1023-1030
[5] Perseguers S, Cirac J I, Acín A, Lewenstein M and Wehr J 2008 *Phys. Rev. A* **77** 022308
[6] DiVincenzo D P, et al, "The entanglement of assistance", in *Lecture Notes in Computer Science* (Springer-Verlag, Berlin, 1999) **1509** 247-257
[7] Laustsen T, Verstraete F and van Enk S J 2003 *Quantum Inf. and Comp.* **3** 64-83
[8] Verstraete F, Popp M and Cirac J I 2004 *Phys. Rev. Lett.* **92** 027901
[9] Popp M, Verstraete F, Martin-Delgado M A and Cirac J I 2005 *Phys. Rev. A* **71** 042306

[10] Gour G 2006 *Phys. Rev. A* **74** 052307
[11] Clerk A A, Devoret M H, Girvin S M, Marquardt F and Schoelkopf R J 2010 *Rev. Mod. Phys.* **82** 1155-1208
[12] Aolita L, Chaves R, Cavalcanti D, Acín A and Davidovich L 2008 *Phys. Rev. Lett.* **100** 080501
[13] Man Z X, Xia Y J and An N B 2008 *Phys. Rev. A* **78** 064301
[14] Huang J H, Wang L G, and Zhu S Y 2010 *Phys. Rev. A* **81** 064304
[15] Zhou J and Guo H 2012 *J. Phys. B: At. Mol. Opt. Phys.* **45** 225503
[16] Perseguers S, Lapeyre Jr G J, Cavalcanti D, Lewenstein M and Acín A 2013 *Rep. Prog. Phys.* **76** 096001.
[17] Greenberger D M, Horne M A, Shimony A and Zeilinger A 1990 Am. J. Phys. **58** 1131-43
[18] Bose S, Vedral V and Knight P L 1998 *Phys Rev A* **57** 822-29
[19] Lu C Y, Yang T and Pan J W 2009 *Phys Rev Lett* **103** 020501
[20] Pagonis C, Redhead M L G, Clifton R K 1991 *Phys. Lett. A* **155** 441-44
[21] Hillery M, Bužek V and Berthiaume A 1999 *Phys. Rev. A* **59** 1829-34
[22] Xiao L, Long G L, Deng F G and Pan J W 2004 *Phys. Rev. A* **69** 052307
[23] Wang X W, Zhang D Y, Tang S Q and Gao F 2010 *Int. J. Quantum Inf.* **8** 1301-14
[24] Nielsen M and Chuang I, Quantum Computation and Quantum Information (Cambridge Univ. Press, Cambridge, 2000).
[25] Zyczkowski K, Horodecki P, Sanpera A and Lewenstein M 1998 *Phys. Rev. A* **58** 883-92
[26] Vidal G and Werner R F 2002 *Phys. Rev. A* **65** 032314
[27] Bennett C H, DiVincenzo D P, Smolin J A and Wootters W K 1996 *Phys. Rev. A* **54** 3824-51
[28] Horodecki M, Horodecki P and Horodecki R 1999 *Phys. Rev. A* **60** 1888-98
[29] Bennett C H, Brassard G, Popescu S, Schumacher B, Smolin J A and Wootters W K 1996 *Phys. Rev. Lett.* **76** 722-725
[30] Horodecki M, Horodecki P and Horodecki R 1997 *Phys. Rev. Lett.* **78** 574-77
[31] Almeida M P, de Melo F, Hor-Meyll M, Salles A, Walborn S P, Souto Ribeiro P H and Davidovich L 2007 *Science* **316** 579-82
[32] Yu T and Eberly J H 2004 *Phys. Rev. Lett.* **93** 140404
[33] Laurat J, Choi K S, Deng H, Chou C W and Kimble H J 2007 *Phys. Rev. Lett.* **99** 180504
[34] Bellomo B, Lo Franco R and Compagno G 2007 *Phys. Rev. Lett.* **99** 160502
[35] Huang J H and Zhu S Y 2007 *Phys. Rev. A* **76** 062322
[36] Badziag P, Horodecki M, Horodecki P and Horodecki R 2000 *Phys. Rev. A* **62** 012311
[37] Bandyopadhyay S 2002 *Phys. Rev. A* **65** 022302
[38] Verstraete F and Verschelde H 2003 *Phys. Rev. Lett.* **90** 097901
[39] Bandyopadhyay S and Ghosh A 2012 *Phys. Rev. A* **86** 020304(R)
[40] Verstraete F and Verschelde H 2002 *Phys. Rev. A* **66** 022307